Appl. Math. Mech. -Engl. Ed., 2008, **29**(10):1263–1278
DOI 10.1007/s10483-008-1002-2

Applied Mathematics and Mechanics (English Edition)

Generalized thermoelastic functionally graded spherically isotropic solid containing a spherical cavity under thermal shock *

M. K. Ghosh[1], M. Kanoria[2]

(1. Department of Mathematics, Serampore College, Serampore, Hooghly-712201, India;
2. Department of Applied Mathematics, University of Calcutta,
92 A. P. C. Road, Kolkata-700009, India)

(Communicated by GUO Xing-ming)

Abstract This paper is concerned with the determination of thermoelastic displacement, stress and temperature in a functionally graded spherically isotropic infinite elastic medium having a spherical cavity, in the context of the linear theory of generalized thermoelasticity with two relaxation time parameters (Green and Lindsay theory). The surface of cavity is stress-free and is subjected to a time-dependent thermal shock. The basic equations have been written in the form of a vector-matrix differential equation in the Laplace transform domain, which is then solved by an eigenvalue approach. Numerical inversion of the transforms is carried out using the Bellman method. Displacement, stress and temperature are computed and presented graphically. It is found that variation in the thermo-physical properties of a material strongly influences the response to loading. A comparative study with a corresponding homogeneous material is also made.

Key words generalized thermoelasticity, functionally graded material (FGM), Green-Lindsay theory, vector-matrix differential equation, Bellman method

Chinese Library Classification O343.6
2000 Mathematics Subject Classification 74F05

Introduction

Physical observations and the results of conventional coupled dynamic thermoelasticity theories involving infinite speed of thermal signals, which are based on the mixed parabolic-hyperbolic governing equations of Biot[1] and Chadwick[2], are mismatched. To make them relevant, generalized thermoelasticity theories have been developed to ensure the finite speed of thermal signals(second sound) in elastic solids. The first generalization proposed by Lord and Shulman[3] involves one relaxation time parameter in the heat flux-temperature gradient relation. In this theory, a flux-rate term has been introduced into Fourier's heat conduction equation in order to formulate it in a generalized form that involves a hyperbolic-type heat transport equation admitting finite speed of thermal signals. Another model is the temperature-rate-dependent theory of thermoelasticity proposed by Green and Lindsay[4], which involves two relaxation time parameters. The theory obeys the Fourier law of heat conduction and asserts that heat propagates with finite speed. Experimental studies by Tzou[5] and Mitra et al.[6]

* Received Feb. 13, 2008 / Revised Jun. 30, 2008
Corresponding author Mridula Kanoria, E-mail: k_mri@yahoo.com

on this theory show that relaxation times play a significant role in cases involving shock wave propagation, laser techniques, a rapidly propagating crack tip, etc. So when there are problems involving very large heat fluxes at short intervals of time, the conventional theory of thermoelasticity fails to be a suitable model and generalized thermoelasticity is the right form of mathematics to apply. The relevant literature has been reviewed by Chandrashekharaiah[7].

Applying the above theories of generalized thermoelasticity, several problems have been solved. To solve a coupled thermoelastic problem, it is customary to choose a suitable thermoelastic potential function, but this approach has certain limitations, as discussed by Bahar and Hetnarski[8]. A fundamental solution in the generalized theory with two relaxation time parameters has been derived by Ezzat[9] for a cylindrical region. Hetnarski and Ignaczak[10] have studied the response of semi-space to a short laser pulse in the context of the generalized theory of thermoelasticity. A one-dimensional problem of generalized thermoelasticity of a disk based on the Lord-Shulman theory has been considered by Bagri and Eslami[11]. Kar and Kanoria[12] have investigated the distribution of generalized stresses due to step input of temperature at the boundary of a spherical hole in a homogeneous isotropic unbounded body. Das and Lahiri[13] have studied a problem of generalized thermoelasticity for the transversely isotropic medium with one relaxation time parameter. The generalized stresses in a homogeneous transversely isotropic annular disc has been investigated by Kanoria and Kar[14]. Ghosh and Kanoria[15] have studied the thermoelastic problem in a spherically isotropic infinite elastic medium having a spherical cavity in the context of the linear theory of generalized thermoelasticity with two relaxation time parameters (Green and Lindsay theory).

Thermal shocks and very high temperatures inevitably give rise to severe thermal stresses causing catastrophic failure of structural components such as aircraft engines, turbines, space vehicles, etc. In order to avoid such type of failures, functionally graded materials are used, as discussed by Aboudi et al.[16] and Wetherhold and Wang[17]. These materials are characterized by a microstructure that is spatially variable on a macroscale, and were developed initially for high temperature applications. In these materials, the spatial variation of thermal and mechanical properties strongly influences the response to loading. Sugano[18] has presented an analytical solution for a one-dimensional transient thermal stress problem of a nonhomogeneous plate where the thermal conductivity and Young's modulus vary exponentially, whereas the Poisson's ratio and the coefficient of linear thermal expansion vary arbitrarily in the direction of thickness. Qian and Batra[19] have studied the problem of a transient thermoelastic deformation of a thick functially graded plate with edges held at a uniform temperature. Lutz and Zimmerman[20] have presented the exact solutions for one-dimensional thermal stresses of a functionally graded sphere in which the elastic modulus and coefficient of linear thermal expansion vary linearly with the radial distance. The exact solution for the axisymmetric thermoelastic problem of a uniformly heated functionally graded transversely isotropic cylindrical shell has been presented by Ye et al.[21], in which the modulus of elasticity and the coefficient of linear thermal expansion vary with the power product form of the radial coordinate variable. Chen et al.[22] have solved the problem of free vibration of a fluid-filled hollow sphere of a FGM with spherical isotropy. The thermo-elasto-dynamic response of a functionally graded spherically isotropic hollow sphere has been investigated analytically by Ding et al.[23], in which the problem is formulated by the introduction of a dependent variable and separation of variables technique. The problem of rotating a piezoceramic spherical shell with a functionally graded property in the exact elasto-electric field has been solved by Chen et al.[24]. Wang and Mai[25] have studied the problem of transient one-dimensional thermal stresses in nonhomogeneous materials, such as plates, cylinders and spheres, using the finite element method. A thermomechanical problem of functionally graded hollow circular cylinders has been solved by Shao et al.[26], in which the material properties are assumed to be temperature independent and vary continuously in the radial direction. Mallik and Kanoria[27] have considered a one-dimensional thermoelastic disturbance in an infinitely isotropic FGM in the context of the generalized the-

ory of thermoelasticity without energy dissipation in the presence of distributed periodically varying heat sources. The material properties under consideration are assumed to vary exponentially with the space variable. The generalized coupled thermoelasticity theories proposed by Lord-Shulman, Green-Lindsay and Green-Naghdi have been combined into a unified formulation introducing unified parameters by Bagri and Eslami[28]. Chen[29] has investigated the distribution of stress in a rotating elastic FGM hollow sphere with spherical isotropy. The problem of solving thermal stresses in a hollow circular cylinder and a hollow sphere of a FGM has been considered by Obata and Noda[30]. Theoretical treatment of a transient thermoelastic problem involving a functionally graded cylindrical panel due to nonuniform heat supply in the circumferential direction has been presented by Ootao and Tanigawa[31].

The main objective of this paper is to study the distribution of thermoelastic displacement, stresses and temperature produced in a functionally graded spherically isotropic infinite elastic medium containing a spherical cavity, in the context of the linear theory of generalized thermoelasticity with two relaxation time parameters(Green and Lindsay model). The surface of the cavity is stress-free and is subjected to a time-dependent thermal shock. The thermal and mechanical properties of the FGM under consideration are assumed to vary with the power of the radial coordinate variable. The eigenvalue approach due to Das et al.[32] is used for the solution of the problem. Numerical solutions of the theoretical results are obtained and presented graphically. A comparison with the corresponding homogeneous material is also made.

1 Basic equations

The equations of motion are[33]

$$\rho\ddot{u}_i = \sigma_{ij,j}, \tag{1}$$

where u_i is the displacement component, the stress tensor σ_{ij} is given by

$$\sigma_{ij} = C_{ijkl}e_{kl} - \beta_{ij}\left(T - T_0 + t_1\dot{T}\right), \tag{2}$$

and the generalized heat conduction equation in the absence of a heat source is

$$\begin{aligned}&\left[\left\{\delta_{1s}K_{ij} + \delta_{2s}\left(K^*_{ij} + K_{ij}\frac{\partial}{\partial t}\right)\right\}T_{,j}\right]_{,i}\\ &= \rho C_E\left[\delta_{1s}\dot{T} + (\delta_{1s}t_2 + \delta_{2s})\ddot{T}\right] + T_0\left(\zeta\delta_{1s} + \delta_{2s}\frac{\partial}{\partial t}\right)\beta_{ij}\dot{e_{ij}},\end{aligned} \tag{3}$$

C_{ijkl} $(i,j,k,l = 1,2,3)$ being the elastic coefficients, e_{kl} $(k,l = 1,2,3)$ the strain components, $\beta_{ij}(i,j = 1,2,3)$ the elastic moduli, T the absolute temperature, T_0 the reference temperature, t_1 and t_2 the relaxation times, K_{ij} the coefficient of thermal conductivity, K^*_{ij} the additional material constant, ρ the mass density, C_E the specific heat of the solid at constant strain and δ_{is} the Kronecker delta.

In equations (2) and (3):

(i) if $t_1 = 0, t_2 = 0, s = 1$ and $\zeta = 0$, then they reduce to the equations of the classical theory of thermo-elasticity(CTE);

(ii) if $t_1 = 0, t_2 = 0, s = 1$ and $\zeta = 1$, then they reduce to the equations of the classical coupled theory of thermo-elasticity(CCTE);

(iii) if $s = 1$ and $\zeta = 1$, then they reduce to the equations of the temperature-rate-dependent thermo-elasticity theory (TRDTE (G-L model));

(iv) if $s = 2$, then they reduce to the equations of thermo-elasticity with energy dissipation (TEWED (G-N model)).

The thermal relaxation times satisfy the inequalities[4]

$$t_1 \geq t_2 > 0 \quad \text{in the case of G-L theory.}$$

For functionally graded materials, the parameters ρ, C_{ijkl}, β_{ij}, K_{ij} and K^*_{ij} are space dependent. Thus, we replace these quantities by $\rho' f(\boldsymbol{r})$, $C'_{ijkl} f(\boldsymbol{r})$, $\beta'_{ij} f(\boldsymbol{r})$, $K'_{ij} f(\boldsymbol{r})$ and $K^{*\prime}_{ij} f(\boldsymbol{r})$ where ρ', C'_{ijkl} etc. are assumed to be constants and $f(\boldsymbol{r})$ is a given nondimensional function of space variable $\boldsymbol{r}$. Then the equations (1), (2) and (3) take the form (dropping primes for convenience):

$$\begin{aligned} f(\boldsymbol{r})\rho\ddot{u}_i = {} & [C_{ijkl}e_{kl} - \beta_{ij}\left(T - T_0 + t_1\dot{T}\right)]_{,j}\, f(\boldsymbol{r}) \\ & + [C_{ijkl}e_{kl} - \beta_{ij}\left(T - T_0 + t_1\dot{T}\right)] f(\boldsymbol{r})_{,j}\,, \end{aligned} \tag{4}$$

$$\sigma_{ij} = [C_{ijkl}e_{kl} - \beta_{ij}\left(T - T_0 + t_1\dot{T}\right)] f(\boldsymbol{r}), \tag{5}$$

$$\begin{aligned} & \left[f(\boldsymbol{r})\left\{\delta_{1s}K_{ij} + \delta_{2s}\left(K^*_{ij} + K_{ij}\frac{\partial}{\partial t}\right)\right\} T_{,j}\right]_{,i} \\ & = \rho C_E f(\boldsymbol{r})\left\{\delta_{1s}\dot{T} + (\delta_{1s}t_2 + \delta_{2s})\ddot{T}\right\} + T_0\left(\zeta\delta_{1s} + \delta_{2s}\frac{\partial}{\partial t}\right)\beta_{ij}\dot{e_{ij}} f(\boldsymbol{r}). \end{aligned} \tag{6}$$

2 Formulation of the problem

We consider a functionally graded spherically isotropic infinite solid having a spherical cavity of radius a. The surface of the cavity is stress-free and is suddenly heated and kept at a temperature that varies with time. We also assume that neither the body forces nor the heat sources are acting inside the medium.

We use spherical polar coordinates (r, θ, ϕ) with the origin at the center of the cavity and we consider those thermoelastic interactions which are spherically symmetric. It follows that the displacement vector $\boldsymbol{u}$ and the temperature T have the forms

$$\begin{cases} \boldsymbol{u} = (u(r,t), 0, 0), \\ T = T(r,t). \end{cases} \tag{7}$$

Then

$$\begin{cases} e_r \equiv e_{rr} = \dfrac{\partial u}{\partial r}, \\ e_\theta \equiv e_{\theta\theta} = e_{\phi\phi} = \dfrac{u}{r}. \end{cases} \tag{8}$$

The stresses in the radial, cross radial and transverse directions are σ_{rr}, $\sigma_{\theta\theta}$ and $\sigma_{\phi\phi}$, respectively, where

$$\begin{cases} \sigma_{rr}(r,t) = \sigma_r(r,t), \\ \sigma_{\theta\theta}(r,t) = \sigma_\theta(r,t) = \sigma_{\phi\phi}(r,t). \end{cases} \tag{9}$$

It is assumed that the material properties depend only on the radial coordinate r. So we can take $f(\boldsymbol{r}) = f(r)$.

In the context of the linear theory of generalized thermoelasticity based on the Green-Lindsay theory, the constitutive equations of the spherically isotropic body are taken as in Ref. [34],

$$\sigma_r = [C_{11}e_r + 2C_{12}e_\theta - \beta_r(T - T_0 + t_1\dot{T})] f(r), \tag{10}$$

$$\sigma_\theta = \sigma_\phi = [C_{12}e_r + (C_{22} + C_{23})e_\theta - \beta_\theta(T - T_0 + t_1\dot{T})] f(r), \tag{11}$$

and $\beta_{ij} = \beta_i \delta_{ij}$ and $K_{ij} = K_i \delta_{ij}$ (i not summed).

The equation of motion (4) in the absence of any body forces becomes

$$\frac{\partial}{\partial r}[C_{11}e_r + 2C_{12}e_\theta - \beta_r(T - T_0 + t_1\dot{T})f(r)] + \frac{2}{r}[C_{11}e_r + 2C_{12}e_\theta - \beta_r(T - T_0 + t_1\dot{T}) - C_{12}e_r - (C_{22} + C_{23})e_\theta + \beta_\theta(T - T_0 + t_1\dot{T})]f(r) = \rho f(r)\frac{\partial^2 u}{\partial t^2}. \tag{12}$$

In the absence of heat sources, the heat conduction equation (6) reduces to (taking $s = 1$ and $\zeta = 1$ for G-L model)

$$\frac{1}{r^2}\frac{\partial}{\partial r}\left[K_r f(r) r^2 \frac{\partial T}{\partial r}\right] = \left[\rho C_E\left(\frac{\partial T}{\partial t} + t_2\frac{\partial^2 T}{\partial t^2}\right) + T_0\frac{\partial}{\partial t}\left(\beta_r\frac{\partial u}{\partial r} + \beta_\theta\frac{2u}{r}\right)\right] f(r). \tag{13}$$

The problem is to solve equations (12) and (13), subject to the boundary conditions:

i) stress-free boundary,

$$\sigma_r(r,t) = 0 \quad \text{on} \quad r = a; \tag{14}$$

and ii) varying thermal load,

$$T(r,t) = T_0\{1 + F(t)\} \quad \text{on} \quad r = a, \tag{15}$$

where $F(t)$ is a known function of time t.

The initial and regularity conditions can be written as

$$\begin{cases} u = 0 = T \text{ at } \ t = 0,\ r \geq a; \\ \dfrac{\partial u}{\partial t} \ = \ 0 \ = \dfrac{\partial T}{\partial t} \ \text{ at } t = 0; \\ u = \ 0 \ = \ T \text{ when } r \to \infty. \end{cases} \tag{16}$$

The following non-dimensional quantities are introduced as

$$\begin{cases} r^* = V\eta r, \quad a^* = V\eta a, \quad u^* = V\eta u, \\ \sigma_{ij}^* = \dfrac{\sigma_{ij}}{C_{11}}, \quad t^* = V^2\eta t, \quad t_1^* = V^2\eta t_1, \\ t_2^* = V^2\eta t_2, \quad T_1 = \dfrac{T - T_0}{T_0}, \end{cases} \tag{17}$$

where $V = \sqrt{(\frac{C_{11}}{\rho})}$, $\eta = \frac{\rho C_E}{K_r}$.

Using these non-dimensional variables and taking $f(r) = f^*(r^*)$, the equations (10)–(13) take the form (dropping the asterisks for convenience):

$$\sigma_r = \left[\frac{\partial u}{\partial r} + \frac{2C_{12}}{C_{11}}\frac{u}{r} - \frac{\beta_r T_0}{C_{11}}\left(T_1 + t_1\frac{\partial T_1}{\partial t}\right)\right] f(r), \tag{18}$$

$$\sigma_\theta = \left[\frac{C_{12}}{C_{11}}\frac{\partial u}{\partial r} + \frac{C_{22} + C_{23}}{C_{11}}\frac{u}{r} - \frac{\beta_\theta T_0}{C_{11}}\left(T_1 + t_1\frac{\partial T_1}{\partial t}\right)\right] f(r), \tag{19}$$

$$\frac{\partial}{\partial r}\left[\left\{\frac{\partial u}{\partial r}+\frac{2C_{12}}{C_{11}}\frac{u}{r}-\frac{\beta_r T_0}{C_{11}}\left(T_1+t_1\frac{\partial T_1}{\partial t}\right)\right\}f(r)\right]$$
$$+\frac{2}{r}\left[\frac{\partial u}{\partial r}+\frac{2C_{12}}{C_{11}}\frac{u}{r}-\frac{\beta_r T_0}{C_{11}}\left(T_1+t_1\frac{\partial T_1}{\partial t}\right)\right]f(r)$$
$$-\frac{2}{r}\left[\frac{C_{12}}{C_{11}}\frac{\partial u}{\partial r}+\frac{C_{22}+C_{23}}{C_{11}}\frac{u}{r}-\frac{\beta_\theta T_0}{C_{11}}\left(T_1+t_1\frac{\partial T_1}{\partial t}\right)\right]f(r)=f(r)\frac{\partial^2 u}{\partial t^2}, \tag{20}$$

$$\frac{\eta}{r^2}\frac{\partial}{\partial r}\left(K_r T_0 f(r) r^2\frac{\partial T_1}{\partial r}\right)$$
$$=\rho T_0 C_E f(r)\left(\frac{\partial T_1}{\partial t}+t_2\frac{\partial^2 T_1}{\partial t^2}\right)+T_0 f(r)\frac{\partial}{\partial t}\left(\beta_r\frac{\partial u}{\partial r}+\beta_\theta\frac{2u}{r}\right). \tag{21}$$

3 Material inhomogeneity (power-law dependence)

We take $f(r)=r^n$, where n is a dimensionless constant. Then, the equations (18)–(21) become

$$\sigma_r=\left[\frac{\partial u}{\partial r}+\frac{2C_{12}}{C_{11}}\frac{u}{r}-\frac{\beta_r T_0}{C_{11}}\left(T_1+t_1\frac{\partial T_1}{\partial t}\right)\right]r^n, \tag{22}$$

$$\sigma_\theta=\left[\frac{C_{12}}{C_{11}}\frac{\partial u}{\partial r}+\frac{C_{22}+C_{23}}{C_{11}}\frac{u}{r}-\frac{\beta_\theta T_0}{C_{11}}\left(T_1+t_1\frac{\partial T_1}{\partial t}\right)\right]r^n, \tag{23}$$

$$\frac{\partial^2 u}{\partial r^2}+\frac{n+2}{r}\frac{\partial u}{\partial r}-2\left[\frac{C_{22}+C_{23}-(n+1)C_{12}}{C_{11}}\right]\frac{u}{r^2}$$
$$-\frac{T_0\beta_r}{C_{11}}\left[\frac{\partial}{\partial r}\left(T_1+t_1\frac{\partial T_1}{\partial t}\right)-\frac{2\left(N-\frac{n+2}{2}\right)}{r}\left(T_1+t_1\frac{\partial T_1}{\partial t}\right)\right]=\frac{\partial^2 u}{\partial t^2}, \tag{24}$$

$$\frac{\partial^2 T_1}{\partial r^2}+\frac{n+2}{r}\frac{\partial T_1}{\partial r}=\frac{\partial T_1}{\partial t}+t_2\frac{\partial^2 T_1}{\partial t^2}+\frac{\beta_r}{K_r\eta}\frac{\partial}{\partial t}\left(\frac{\partial u}{\partial r}+\frac{2Nu}{r}\right), \tag{25}$$

where $N=\frac{\beta_\theta}{\beta_r}$.

4 Formation of vector-matrix differential equation in the Laplace transform domain

Let us define Laplace transform of a function $g(r,t)$ by

$$\overline{g}(r,p)=\int_0^\infty g(r,t)\mathrm{e}^{-pt}dt, \tag{26}$$

with $Re(p)>0$.

On taking the Laplace transform of both sides of equations (22)–(25), we get

$$\bar{\sigma_r}=\left[\frac{d\bar{u}}{dr}+\frac{2C_{12}}{C_{11}}\frac{\bar{u}}{r}-\frac{\beta_r T_0}{C_{11}}(1+t_1 p)\bar{T_1}\right]r^n, \tag{27}$$

$$\bar{\sigma_\theta}=\left[\frac{C_{12}}{C_{11}}\frac{d\bar{u}}{dr}+\frac{C_{22}+C_{23}}{C_{11}}\frac{\bar{u}}{r}-\frac{N\beta_r T_0}{C_{11}}(1+t_1 p)\bar{T_1}\right]r^n, \tag{28}$$

$$\frac{d^2\bar{u}}{dr^2}+\frac{n+2}{r}\frac{d\bar{u}}{dr}-2\left[\frac{C_{22}+C_{23}-(n+1)C_{12}}{C_{11}}\right]\frac{\bar{u}}{r^2}$$
$$-\frac{T_0\beta_r(1+t_1p)}{C_{11}}\left[\frac{d}{dr}-\frac{2(N-\frac{n+2}{2})}{r}\right]\bar{T}_1=p^2\bar{u}, \tag{29}$$

$$\frac{d^2\bar{T}_1}{dr^2}+\frac{n+2}{r}\frac{d\bar{T}_1}{dr}=p(1+t_2p)\bar{T}_1+\frac{p\beta_r}{K_r\eta}\left(\frac{d\bar{u}}{dr}+2N\frac{\bar{u}}{r}\right). \tag{30}$$

Let us assume $N=\frac{n+2}{2}$. Then equation (29) becomes

$$\frac{d^2\bar{u}}{dr^2}+\frac{n+2}{r}\frac{d\bar{u}}{dr}-\frac{2}{r^2}\left[\frac{C_{22}+C_{23}-(n+1)C_{12}}{C_{11}}\right]\bar{u}=p^2\bar{u}+\frac{T_0\beta_r(1+t_1p)}{C_{11}}\frac{d\bar{T}_1}{dr}, \tag{31}$$

and differentiating equation (30) with respect to r, we get

$$\frac{d^2}{dr^2}\left(\frac{d\bar{T}_1}{dr}\right)+\frac{n+2}{r}\frac{d}{dr}\left(\frac{d\bar{T}_1}{dr}\right)-\frac{2}{r^2}\left[\frac{C_{22}+C_{23}-(n+1)C_{12}}{C_{11}}\right]\frac{d\bar{T}_1}{dr}$$
$$=\left[\frac{p^3\beta_r}{K_r\eta}+\frac{2}{r^2}\left\{\frac{C_{22}+C_{23}-(n+1)C_{12}-\frac{n+2}{2}C_{11}}{C_{11}}\right\}\right]\bar{u}$$
$$+\left[\frac{pT_0{\beta_r}^2(1+t_1p)}{K_r\eta C_{11}}+p(1+t_2p)-\frac{2}{r^2}\left\{\frac{C_{22}+C_{23}-(n+1)C_{12}-\frac{n+2}{2}C_{11}}{C_{11}}\right\}\right]\frac{d\bar{T}_1}{dr}. \tag{32}$$

The coupled equations (31) and (32) can be put in a vector-matrix differential equation as follows:

$$L\tilde{V}=\tilde{A}\tilde{V}, \tag{33}$$

where

$$L\equiv\frac{d^2}{dr^2}+\frac{n+2}{r}\frac{d}{dr}-\frac{2m+n+2}{r^2}, \tag{34}$$

$$\tilde{V}\equiv\begin{bmatrix}\bar{u}\\ \frac{d\bar{T}_1}{dr}\end{bmatrix}, \tag{35}$$

$$\tilde{A}\equiv\begin{bmatrix}b & c\\ bd & cd+f\end{bmatrix}, \tag{36}$$

$$\begin{cases} m\equiv\dfrac{C_{22}+C_{23}-\{\frac{n+2}{2}C_{11}+(n+1)C_{12}\}}{C_{11}}, \quad b\equiv p^2, \quad c\equiv\dfrac{T_0\beta_r}{C_{11}}(1+t_1p),\\ d\equiv\dfrac{p\beta_r}{\rho C_E}=\dfrac{p\beta_r}{K\eta}, \quad f\equiv p(1+t_2p), \quad n=2\dfrac{C_{22}+C_{23}-(C_{11}+C_{12})}{C_{11}+2C_{12}}. \end{cases} \tag{37}$$

The problem is to solve the equation (33) subject to the boundary conditions (14) and (15) with

$$F(t)=\theta_0[H(t)-H(t-t_0)] \quad \text{on} \quad r=a,$$

where $H(t)$ is the Heaviside unit step function and t_0 is the short time during which the shock is applied.

Applying Laplace transform to these boundary conditions, we obtain

$$\bar{\sigma}_r(a,p)=0 \tag{38}$$

and

$$\bar{T}_1(a,p)=\frac{\theta_0}{p}(1-\mathrm{e}^{-pt_0}). \tag{39}$$

5 Method of solution

To solve equation (33), we substitute

$$\tilde{V} = \tilde{X}(\lambda) w(r, \lambda), \tag{40}$$

where λ is a scalar, $w(r, \lambda)$ is a non-trivial solution of the scalar differential equation:

$$\frac{d^2 w}{dr^2} + \frac{n+2}{r}\frac{dw}{dr} - \frac{2m+n+2}{r^2} w = \lambda^2 w, \tag{41}$$

and the vector $\tilde{X}(\lambda)$ is independent of r and satisfies

$$\tilde{A}\tilde{X}(\lambda) = \lambda^2 \tilde{X}(\lambda). \tag{42}$$

As a solution of equation (33) that is consistent with the problem, we can have

$$\tilde{V}(r, p) = r^{-\frac{n+1}{2}} \sum_{i=1}^{2} A_i \tilde{X}(\lambda_i) \left[\frac{1}{\lambda_i^2} K_h(\lambda_i r) \right], \tag{43}$$

where

$$h^2 = 2m + n + 2 + \left(\frac{n+1}{2} \right)^2, \tag{44}$$

$K_h(\lambda_i r)$ being the modified Bessel function of the second kind of order h, and $A_i (i = 1, 2)$ are constants to be determined from the boundary conditions.

Now the characteristic equation corresponding to the matrix $\tilde{A}$ is written as

$$\lambda^4 - (b + cd + f)\lambda^2 + fb = 0. \tag{45}$$

The eigen vectors $\tilde{X}(\lambda_i)$ $(i = 1, 2)$ corresponding to the eigen values λ_i^2 $(i = 1, 2)$ can be obtained as

$$\tilde{X}(\lambda_i) = \begin{bmatrix} X_1(\lambda_i) \\ X_2(\lambda_i) \end{bmatrix} = \begin{bmatrix} -c \\ b - \lambda_i^2 \end{bmatrix}, \quad i = 1, 2. \tag{46}$$

The components of the vector $\tilde{V}$ can now be written as

$$\bar{u}(r, p) = -r^{-\frac{n+1}{2}} \sum_{i=1}^{2} cA_i \left[\frac{1}{\lambda_i^2} K_h(\lambda_i r) \right], \tag{47}$$

$$\frac{d\bar{T}_1(r, p)}{dr} = r^{-\frac{n+1}{2}} \sum_{i=1}^{2} (b - \lambda_i^2) A_i \left[\frac{1}{\lambda_i^2} K_h(\lambda_i r) \right]. \tag{48}$$

Hence

$$\bar{\sigma}_r(r, p) = \left(\frac{cA_1}{\lambda_1^2} \right) QR_1 + \left(\frac{cA_2}{\lambda_2^2} \right) QR_2, \tag{49}$$

$$\bar{\sigma}_\theta(r, p) = \left(\frac{cA_1}{\lambda_1^2} \right) QR1_1 + \left(\frac{cA_2}{\lambda_2^2} \right) QR1_2, \tag{50}$$

$$\bar{T}_1(r, p) = \left(\frac{cA_1}{\lambda_1^2} \right) \frac{SR_1}{c} + \left(\frac{cA_2}{\lambda_2^2} \right) \frac{SR_2}{c}, \tag{51}$$

where

$$QR_i = \left[\left(\frac{n+1}{2} - 2\frac{C_{12}}{C_{11}}\right) K_h(\lambda_i r)\right] r^{\frac{n-3}{2}} - \left[\lambda_i r \frac{d}{d(\lambda_i r)}\{K_h(\lambda_i r)\}\right] r^{\frac{n-3}{2}} + \left[(b-\lambda_i^2) r^{\frac{n+3}{2}} \int_r^\infty u^{-\frac{n+1}{2}} K_h(\lambda_i u) du\right] r^{\frac{n-3}{2}} \quad \text{for} \quad i = 1, 2; \tag{52}$$

$$QR1_i = \left[\left(\frac{n+1}{2}\frac{C_{12}}{C_{11}} - \frac{C_{22}+C_{23}}{C_{11}}\right) K_h(\lambda_i r)\right] r^{\frac{n-3}{2}} - \left[\lambda_i \frac{C_{12}}{C_{11}} r \frac{d}{d(\lambda_i r)}\{K_h(\lambda_i r)\}\right] r^{\frac{n-3}{2}} + \left[(b-\lambda_i^2) r^{\frac{n+3}{2}} \int_r^\infty u^{-\frac{n+1}{2}} K_h(\lambda_i u) du\right] r^{\frac{n-3}{2}}, \quad \text{for} \quad i = 1, 2; \tag{53}$$

$$SR_i = -(b-\lambda_i^2) \int_r^\infty u^{-\frac{n+1}{2}} K_h(\lambda_i u) du, \quad \text{for} \quad i = 1, 2; \tag{54}$$

$$\frac{cA_1}{\lambda_1^2} = -\frac{c\theta_0 \left(1 - \mathrm{e}^{-pt_0}\right) QA_2}{D}; \tag{55}$$

$$\frac{cA_2}{\lambda_2^2} = \frac{c\theta_0 \left(1 - \mathrm{e}^{-pt_0}\right) QA_1}{D}; \tag{56}$$

$$D = p(QA_1 SA_2 - SA_1 QA_2); \tag{57}$$

$$\begin{cases} QA_i = [QR_i]_{r=a}, & i = 1, 2; \\ SA_i = [SR_i]_{r=a}, & i = 1, 2. \end{cases} \tag{58}$$

The results for a homogeneous material[15] can be deduced from this solution by putting $n = 0$ as a case in particular.

6 Numerical results and discussion

To obtain the solution of the problem in the physical domain, we must invert the transforms in equations (47), (49)–(51). Here, we adopt the method of Bellman et al.[35] for inversion and choose a time span given by seven values of time t_i, $i = 1$ to 7 (Appendix A), at which σ_r, σ_θ and T_1 are evaluated from the negative of logarithms of the roots of the shifted Legendre polynomial of degree seven.

The materials chosen for numerical calculation are steel, magnesium and zinc, for which the values of the nonhomogeneous parameter n are $0.0, 0.05$ and 1.0, respectively. The associated constants are taken as

$$t_0 = 0.1 \text{ s}, \quad T_0 = 296 \text{ K}, \quad \theta_0 = 1.0;$$

and for steel $(n = 0.0)$[34] :

$$\begin{aligned} &C_{11} = 0.27865 \times 10^{12} \text{ Pa}, && C_{12} = 0.11942 \times 10^{12} \text{ Pa}, \\ &C_{22} = 0.27865 \times 10^{12} \text{ Pa}, && C_{23} = 0.11942 \times 10^{12} \text{ Pa}, \\ &\rho = 0.78 \times 10^4 \text{ kg/m}^3, && C_E = 117 \text{ J/(kg} \cdot \text{K)}, \\ &\beta_r = 5.5889 \times 10^6 \text{ Pa/K}, && K_r = 59.0 \text{ W/(m} \cdot \text{K)}, \\ &t_1 = 0.75 \times 10^{-13} \text{ s}, && t_2 = 0.5 \times 10^{-13} \text{ s}; \end{aligned}$$

for magnesium $(n = 0.05)$[36] :

$$C_{11} = 0.617 \times 10^{11} \text{ Pa}, \quad C_{12} = 0.217 \times 10^{11} \text{ Pa}$$
$$C_{22} = 0.5974 \times 10^{11} \text{ Pa}, \quad C_{23} = 0.2624 \times 10^{11} \text{ Pa},$$
$$\rho = 0.174 \times 10^{4} \text{ kg/m}^3, \quad C_E = 1040 \text{ J/(kg} \cdot \text{K)}$$
$$\beta_r = 2.68 \times 10^{6} \text{ Pa/K}, \quad K_r = 170.0 \text{ W/(m} \cdot \text{K)},$$
$$t_1 = 0.75 \times 10^{-13} \text{ s}, \quad t_2 = 0.5 \times 10^{-13} \text{ s};$$

and for zinc $(n = 1.0)$[36]:

$$C_{11} = 0.627 \times 10^{11} \text{ Pa}, \quad C_{12} = 0.508 \times 10^{11} \text{ Pa},$$
$$C_{22} = 1.628 \times 10^{11} \text{ Pa}, \quad C_{23} = 0.362 \times 10^{11} \text{ Pa},$$
$$\rho = 0.714 \times 10^{4} \text{ kg/m}^3, \quad C_E = 390 \text{ J/(kg} \cdot \text{K)},$$
$$\beta_r = 5.75 \times 10^{6} \text{ Pa/K}, \quad K_r = 124.0 \text{ W/(m} \cdot \text{K)},$$
$$t_1 = 0.75 \times 10^{-13} \text{ s}, \quad t_2 = 0.5 \times 10^{-13} \text{ s}.$$

Figure 1 depicts the change in radial displacement u versus radial distance r for time $t = 0.14$ and for different values of the non-homogeneous parameter $n(= 0.0, 0.05, 1.0)$. It is seen that in each of the three cases, u attains its maximum value near the surface of the cavity and it vanishes at large r. Also, it increases with the increase in n. The effect of thermal shock in u with t near the surface of the cavity is shown in Figure 2, for $n = 0.0, 0.05$ and 1.0. As may be seen from the figure, each u is of oscillatory nature and its sign is changed when it gets reflected by the elastic wave from the other direction.

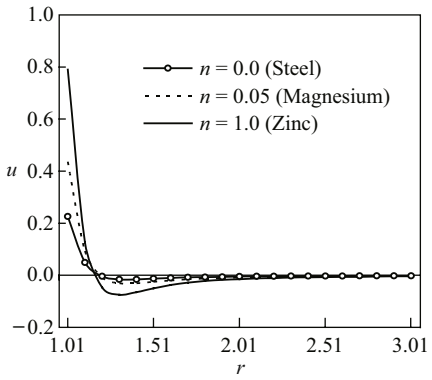

Fig. 1 Radial displacement vs. radial distance (for different values of n and for $t = 0.14$)

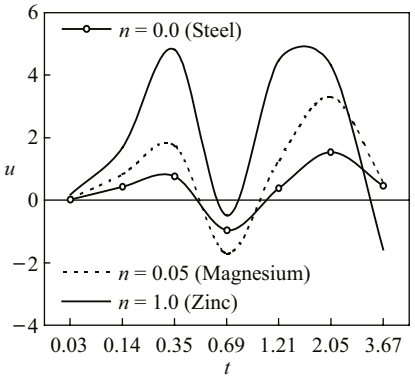

Fig. 2 Radial displacement vs. time (for different values of n and for $r = 1.5$)

Figure 3 represents the graph of u versus r for $n = 0.0, 1.0$ and $t = 0.14, 3.67$. It is seen that the magnitude of u increases as t increases for a fixed n, and also when n increases for a fixed t. Figure 4 shows the variation of u with t for $n = 0.0, 1.0$ and $r = 1.5, 3.0$. It is noted that propagation of u occurs when $r = 3.0$, whereas $r = 1.5$ corresponds to reflection.

Figure 5 shows the variation of radial stress σ_r versus radial distance r for time $t = 0.14$ when the nonhomogeneous parameter $n = 0.0, 0.05$ and 1.0. It is observed that σ_r vanishes at $r = 1$, satisfying the theoretical condition, and it increases with an increase in n for a fixed r. It is also seen that in each case, σ_r decreases with the increase in r, which is physically plausible.

Figure 6 is plotted to show the variation of σ_r versus t for $r = 1.5$ when $n = 0.0, 0.05$ and 1.0. It is seen that for each n, σ_r is negative when t is least showing its compressive nature at the primary stage of load application. In this case, the magnitude of σ_r is found to be maximum for $n = 1.0$, for any r $(1.0 \leq r \leq 3.0)$. Figure 7 represents the graph of σ_r versus r for $n = 0.0, 1.0$ and $t = 0.14, 3.67$. It is noted that the magnitude of σ_r increases when t increases for a fixed n and also when n increases for a fixed t. Thus, the presence of the nonhomogeneous parameter leads to stress amplification. Figure 8 is plotted to show the variation of σ_r against t for $n = 0.0, 1.0$ and $r = 1.5, 3.0$. It is evident that σ_r is compressive in each case for the least value of t. The oscillatory nature of σ_r is found as r increases about the line $\sigma_r = 0$ with decreasing amplitude for each n.

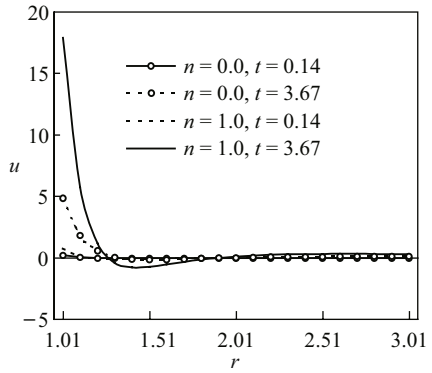

Fig. 3 Radial displacement vs. radial distance (for $n = 0.0$, 1.0 and $t = 0.14$, 3.67)

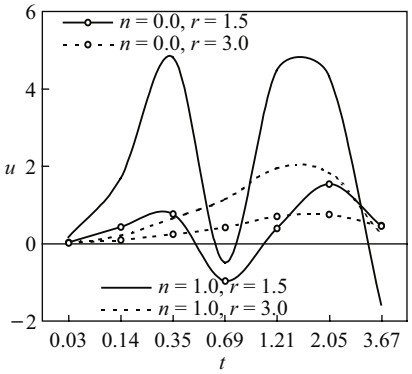

Fig. 4 Radial displacement vs. time (for $n = 0.0$, 1.0 and $r = 1.5$, 3.0)

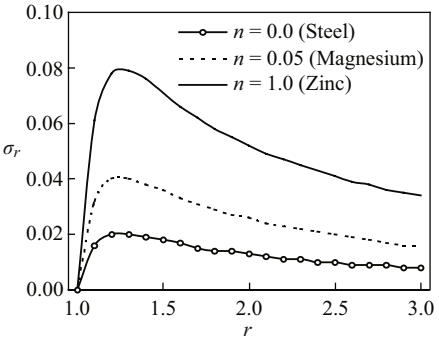

Fig. 5 Radial stress vs. radial distance (for different values of n and for $t = 0.14$)

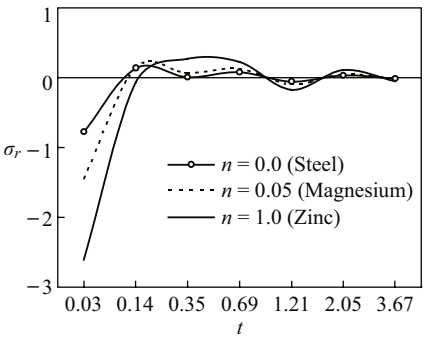

Fig. 6 Radial stress vs. time (for different values of n and for $r = 1.5$)

The hoop stress σ_θ is plotted against r in Figure 9 for the same parameters as in Fig. 5. It is seen that σ_θ increases as n increases, keeping r fixed. In each case σ_θ vanishes at large r. Figure 10 represents the graph of σ_θ versus t for $r = 1.5$ and $n = 0.0, 0.05$ and 1.0. It is seen that σ_θ is compressive when t is least, which is true under temperature pulse and which agrees with the assumed temperature condition. The oscillatory nature of σ_θ is observed for each n; also, the magnitude of σ_θ decreases as t increases for each n. As in Figure 9, here also, for specific t, $|\sigma_\theta|$ increases as n increases. Figure 11 represents the graph of σ_θ versus r for $n = 0.0, 1.0$ and $t = 0.14$, 3.67. It is observed that for a fixed t, the magnitude of σ_θ can be

increased by changing n from 0.0 to $n = 1.0$. Also, when r is fixed, stress amplification occurs in both cases when $n = 1.0$ and $t = 3.67$. However, in all cases, its magnitude decreases as r increases. Figure 12 is plotted for σ_θ against t for $n = 0.0, 1.0$ and $r = 1.5, 3.0$. In all cases, the stresses are compressive for the least value of t. For any value of n and r, the oscillatory nature of the stress is observed about the line $\sigma_\theta = 0$ and its magnitude decreases with an increase in t.

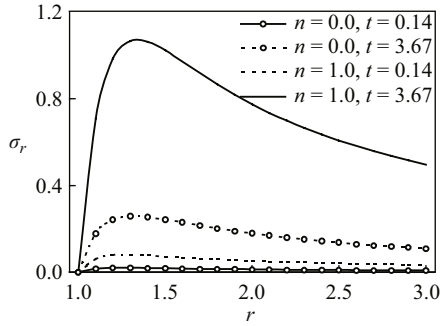

Fig. 7 Radial stress vs. radial distance (for $n = 0.0$, 1.0 and $t = 0.14$, 3.67)

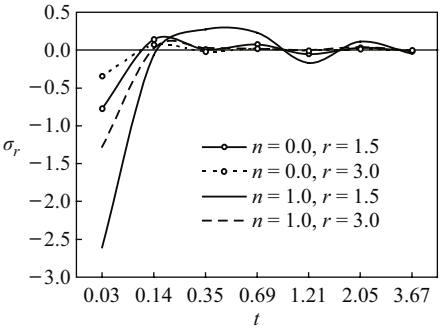

Fig. 8 Radial stress vs. time (for $n = 0.0$, 1.0 and $r = 1.5$, 3.0)

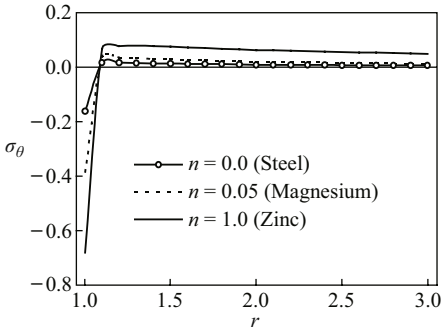

Fig. 9 Hoop stress vs. radial distance (for different values of n and for $t = 0.14$)

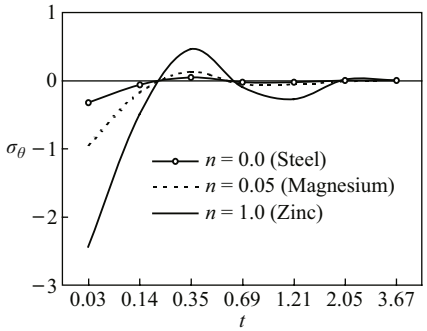

Fig. 10 Hoop stress vs. time (for different values of n and for $r = 1.5$)

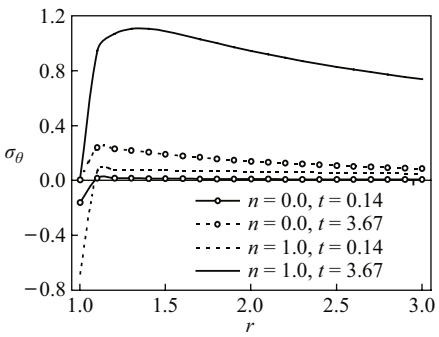

Fig. 11 Hoop stress vs. radial distance (for $n = 0.0$, 1.0 and $t = 0.14$, 3.67)

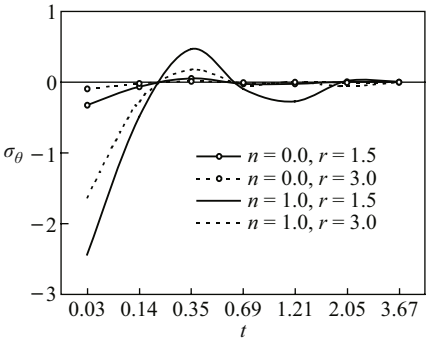

Fig. 12 Hoop stress vs. time (for $n = 0.0$, 1.0 and $r = 1.5$, 3.0)

Figure 13 gives a comparison between the temperatures generated in the bodies corresponding to $n = 0.0$ and $n = 1.0$ for two different values of time $t = 0.69$ and $t = 2.05$. It is observed that for a fixed r and t, the homogeneous property of the material induces T_1 to be maximum. Also in each case, T_1 is found to attain its maximum value near the source. Figure 14 represents the graph of T_1 against t for $n = 0.0, 1.0$ and $r = 1.5, 3.0$. It is seen that for a fixed n and r, the magnitude of T_1 is greatest when t is least. When t increases T_1 oscillates with smaller amplitudes about the line $T_1 = 0$ and it vanishes at large t. Also, when r is fixed, $n = 0.0$ corresponds to temperature amplification.

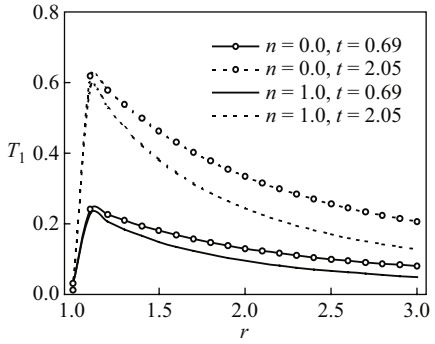

Fig. 13 Temperature vs. radial distance (for $n = 0.0$, 1.0 and $t = 0.69$, 2.05)

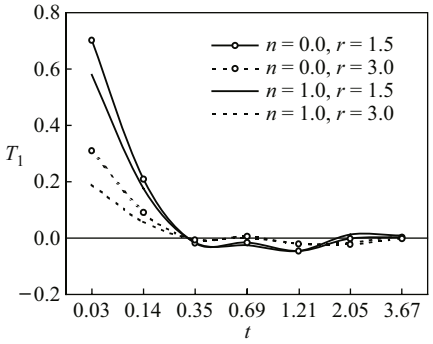

Fig. 14 Temperature vs. time (for $n = 0.0$, 1.0 and $r = 1.5$, 3.0)

7 Conclusions

The problem of investigating the thermoelastic displacement, stresses and temperature produced in a functionally graded spherically isotropic infinite medium containing a spherical cavity under time-dependent thermal shock is studied in the light of the generalized theory of thermoelasticity with two relaxation time parameters(Green and Lindsay theory). The method of Laplace transform is used to write down the basic equations in the form of a vector-matrix differential equation, which is solved by the eigen value approach. The Bellman method is used to get the numerical inversion of the transforms. The thermo-physical parameters are assumed to vary as the power-law exponent of the radial coordinate. The analysis of the results permits some concluding remarks:

1) The thermoelastic displacement, stresses and temperature have a strong dependency on the nonhomogeneous parameter n. So to design an FGM, the importance of the parameter must be taken into consideration.

2) From the figures it is clear that stress amplification occurs when n increases.

3) Both the stresses σ_r and σ_θ are compressive for the least value of time t (figures 6 and 10) and are of oscillatory nature with decreasing amplitude as time progresses.

4) The temperature T_1 produced in a homogeneous body is greater than that produced in a nonhomogeneous body.

Acknowledgements We are grateful to Prof. S. C. Bose of the Department of Applied Mathematics, University of Calcutta for his kind help and guidance in preparation of the paper. We also thank the reviewer for his valuable suggestions for the improvement of the paper.

References

[1] Biot M A. Thermoelasticity and irreversible thermodynamics[J]. *J Appl Phys*, 1956, **27**(3):240–253.

[2] Chadwick P. Progress in solid mechanics[M]. Vol I. Hill R, Sneddon I N (eds). Amsterdam: North Holland, 1960.

[3] Lord H, Shulman Y. A generalized dynamical theory of thermoelasticity[J]. *Mech Phys Solid*, 1967, **15**(5):299–309.

[4] Green A E, Lindsay K A. Thermoelasticity[J]. *J Elast*, 1972, **2**(1):1–7.

[5] Tzou D Y. Experimental support for the lagging behavior in heat propagation[J]. *J Thermophys Heat Transf*, 1995, **9**(4):686–693.

[6] Mitra K, Kumar S, Vedaverg A. Experimental evidence of hyperbolic heat conduction in processed meat[J]. *J Heat Transfer* (*ASME*), 1995, **117**(3):568–573.

[7] Chandrasekharaiah D S. Thermoelasticity with second sound[J]. *A Review Appl Mech Rev*, 1986, **39**(3):355–375.

[8] Bahar L, Hetnarski R. State space approach to thermoelasticity[J]. *J Thermal Stresses*, 1978, **1**(1):135–145.

[9] Ezzat M. Fundamental solution in thermoelasticity with two relaxation times for cylindrical regions[J]. *Int J Eng Sci*, 1995, **33**(14):2011–2020.

[10] Hetnarski R B, Ignaczak J. Generalized thermoelasticity response of semi-space to a short laser pulse[J]. *J Thermal Stresses*, 1994, **17**(3):377–396.

[11] Bagri A, Eslami M R. Generalized coupled thermoelasticity of disks based on the Lord-Shulman model[J]. *J Thermal Stresses*, 2004, **27**(8):691–704.

[12] Kar A, Kanoria M. Thermo-elastic interaction with energy dissipation in an unbounded body with a spherical hole[J]. *International Journal of Solids and Structures*, 2007, **44**(9):2961–2971.

[13] Das N C, Lahiri A. Thermoelastic interactions due to prescribed pressure inside a spherical cavity in an unbounded medium[J]. *Ind J Pure Appl Math*, 2000, **31**(1):19–32.

[14] Kanoria M, Kar A. Thermoelastic interaction with energy dissipation in a transversely isotropic thin circular disc[C]. *Proceedings of the Seventh International Congress on Thermal Stresses*, 2007, 557–560.

[15] Ghosh M K, Kanoria M. Generalized thermoelastic problem of a spherically isotropic infinite elastic medium containing a spherical cavity[J]. *J Thermal Stresses*, 2008, **31**(8):665–679.

[16] Aboudi J, Pindera M J, Arnold S M. Thermo-inelastic response of functionally graded composites[J]. *International Journal of Solids and Structures*, 1995, **32**(12):1675–1710.

[17] Wetherhold R C, Wang S S. The use of functionally graded materials to eliminate or control thermal deformation[J]. *Composites Science and Technology*, 1996, **28**:1099–1104.

[18] Sugano Y. An expression for transient thermal stress in a nonhomogeneous plate with temperature variation through thickness[J]. *Ingenieur Archiv*, 1987, **57**(2):147–156.

[19] Qian L F, Batra R C. Transient thermoelastic deformations of a thick functionally graded plate[J]. *J Thermal Stresses*, 2004, **27**(8):705–740.

[20] Lutz M P, Zimmerman R W. Thermal stresses and effective thermal expansion coefficient of a functionally graded sphere[J]. *J Thermal Stresses*, 1996, **19**(1):39–54.

[21] Ye G R, Chen W Q, Cai J B. A uniformly heated functionally graded cylindrical shell with transverse isotropy[J]. *Mechanics Research Communication*, 2001, **28**(5):535–542.

[22] Chen W Q, Wang X, Ding H J. Free vibration of a fluid-filled hollow sphere of a functionally graded material with spherical isotropy[J]. *Journal of the Acoustical Society of America*, 1999, **106**(5):2588–2594.

[23] Ding H J, Wang H M, Chen W Q. Analytical thermo-elastodynamic solutions for a nonhomogeneous transversely isotropic hollow sphere[J]. *Archive of Applied Mechanics*, 2002, **72**(8):545–553.

[24] Chen W Q, Ding H J, Wang X. The exact elasto-electric field of a rotating piezoceramic spherical shell with a functionally graded property[J]. *International Journal of Solids and Structures*, 2001, **38**(38/39):7015–7027.

[25] Wang B L, Mai Y W. Transient one dimensional heat conduction problems solved by finite element[J]. *International Journal of Mechanical Sciences*, 2005, **47**(2):303–317.

[26] Shao Z S, Wang T J, Ang K K. Transient thermo-mechanical analysis of functionally graded hollow circular cylinders[J]. *J Thermal Stresses*, 2007, **30**(1):81-104.

[27] Mallik S H, Kanoria M. Generalized thermo-elastic functionally graded solid with a periodically varying heat source[J]. *International Journal of Solids and Structures*, 2007, **44**(22/23):7633–7645.

[28] Bagri A, Eslami M R. A unified generalized thermoelasticity formulation; application to thick functionally graded cylinders[J]. *J Thermal Stresses*, 2007, **30**(9/10):911–930.

[29] Chen W Q. Stress distribution in a rotating elastic functionally graded material hollow sphere with spherical isotropy[J]. *Journal of Strain Analysis for Engineering Design*, 2000, **35**(1):13–20.

[30] Obata Y, Noda N. Steady thermal stresses in a hollow circular cylinder and a hollow sphere of a functionally graded material[J]. *J Thermal Stresses*, 1994, **17**(5):471–487.

[31] Ootao Y, Tanigawa Y. Transient thermoelastic problem of a functionally graded cylindrical panel due to nonuniform heat supply[J]. *J Thermal Stresses*, 2007, **30**(5):441–457.

[32] Das N C, Lahiri A, Sen P K. Eigenvalue approach to three dimensional generalized thermoelasticity[J]. *Bulletin Calcutta Math Soc*, 2006, **98**(4):305–318.

[33] Nowacki W. Dynamic problems of thermoelasticity[M]. Warszawa: Polish Scientific Publishers, 1975.

[34] Wang H M, Ding H J, Chen Y M. Thermoelastic dynamic solution of a multilayered spherically isotropic hollow sphere for spherically symmetric problems[J]. *Acta Mechanica*, 2005, **173**(1/4):131–145.

[35] Bellman R, Kolaba R E, Lockette J A. Numerical inversion of the Laplace transform[M]. New York: American Elsevier Pub Co, 1966.

[36] Dhaliwal R S, Sing A. Dynamic coupled thermoelasticity[M]. Delhi: Hindustan Publ, 1980.

Appendix A

Let the Laplace transform of $\sigma_j(R,\eta)$ be given by

$$\overline{\sigma}_j(R,p) = \int_0^\infty \mathrm{e}^{-p\eta}\sigma_j(R,\eta)d\eta. \tag{A.1}$$

We assume that $\sigma_j(R,\eta)$ is sufficiently smooth to permit the use of the approximate method we apply.

Putting $x = \mathrm{e}^{-\eta}$ in equation (A.1), we obtain

$$\overline{\sigma}_j(R,p) = \int_0^1 x^{p-1}g_j(R,x)dx, \tag{A.2}$$

where

$$g_j(R,x) = \sigma_j(R,-\log x). \tag{A.3}$$

Applying the Gaussian quadrature rule to the equation (A.2) we obtain the approximate relation:

$$\sum_{i=1}^{n} W_i x_i^{p-1} g_j(R,x_i) = \overline{\sigma}_j(R,p), \tag{A.4}$$

where x_i $(i = 1,2,\cdots,n)$ are the roots of the shifted Legendre polynomial and W_i $(i = 1,2,\cdots,n)$ are the corresponding weights[35] and $p = 1(1)n$.

For $p = 1(1)n$, equations (A.4) can be written as

$$\begin{aligned}
&W_1 g_j(R,x_1) + W_2 g_j(R,x_2) + \cdots + W_n g_j(R,x_n) = \overline{\sigma}_j(R,1),\\
&W_1 x_1 g_j(R,x_1) + W_2 x_2 g_j(R,x_2) + \cdots + W_n x_n g_j(R,x_n) = \overline{\sigma}_j(R,2),\\
&\quad\cdots\\
&W_1 x_1^{n-1} g_j(R,x_1) + W_2 x_2^{n-1} g_j(R,x_2) + \cdots + W_n x_n^{n-1} g_j(R,x_n) = \overline{\sigma}_j(R,n).
\end{aligned}$$

Therefore,

$$\begin{pmatrix} g_j(R,x_1) \\ g_j(R,x_2) \\ \vdots \\ g_j(R,x_n) \end{pmatrix} = \begin{pmatrix} W_1 & W_2 & \cdots & W_n \\ W_1x_1 & W_2x_2 & \cdots & W_nx_n \\ \vdots & \vdots & \vdots & \vdots \\ W_1x_1^{n-1} & W_2x_2^{n-1} & \cdots & W_nx_n^{n-1} \end{pmatrix}^{-1} \begin{pmatrix} \overline{\sigma}_j(R,1) \\ \overline{\sigma}_j(R,2) \\ \vdots \\ \overline{\sigma}_j(R,n) \end{pmatrix}. \tag{A.5}$$

Hence $g_j(R,x_1)$, $g_j(R,x_2)$, $\cdots$, $g_j(R,x_n)$ can be computed.

For $n=7$ we have x_i and W_i given in Table 1.

Table 1 Roots of the shifted Legendre polynomial and corresponding weights for $n=7$

i	Roots of the shifted Legendre polynomial	Corresponding weights
1	2.5446043828620886E−2	6.4742483084434816E−2
2	1.2923440720030282E−1	1.3985269574463828E−1
3	2.9707742431130145E−1	1.9091502525255938E−1
4	5.0000000000000000E−1	2.0897959183673466E−1
5	7.0292257568869853E−1	1.9091502525255938E−1
6	8.7076559279969706E−1	1.3985269574463828E−1
7	9.7455395617137909E−1	6.4742483084434816E−2

From equations in (A.5) we can calculate the discrete values of $g_j(R,x_i)$, i.e., $\sigma_j(R,\eta_i)$ $(i=1,2,\cdots,7)$; and finally using interpolation we obtain the stress components $\sigma_i(R,\eta)$ $(i=r,\theta)$.